JOURNAL OF SOLID STATE CHEMISTRY **133,** 152–155 (1997)
ARTICLE NO. SC977335

Electron Energy-Loss Spectroscopy Study of the Electronic Structure of Li- and V-Doped β-Rhombohedral Boron

Masami Terauchi, Yosuke Kawamata, Michiyoshi Tanaka, Hirofumi Matsuda,* and Kaoru Kimura*

*Research Institute for Scientific Measurements, Tohoku University, 2-1-1 Katahira Aoba-ku, Sendai 980, Japan; and *Department of Materials, The University of Tokyo, 7-3-1 Hongo, Bunkyo-ku, Tokyo 113, Japan*

Received January 30, 1997; accepted February 12, 1997

Electron energy-loss spectra of Li- and V-doped β-rhombohedral boron (β-r-B) were measured from perfect crystalline areas of 180 nm in diameter. The onset of spectra of Li-doped β-r-B was observed at about 1.5 eV, but that of V-doped β-r-B was not clearly observed. The volume plasmon peaks of Li- and V-doped β-r-B were observed at 23.1 and 23.6 eV, respectively. The energy onset of the B K-shell excitation spectra of V-doped β-r-B was lower than that of β-r-B by 0.9 eV. The lower onset indicates a decrease of the band gap energy with V-doping. Such a decrease of the energy onset was not observed in Li-doped β-r-B.

INTRODUCTION

β-Rhombohedral-boron (β-r-B) consists of 105 boron atoms (B_{105}) in a rhombohedral unit cell and contains B_{12} icosahedral clusters (1). There are three different types of doping sites in the unit cell. It was reported that occupancies of the three doping sites are different for different doping atoms (2–4). Since B_{12} clusters in β-r-B lack two electrons to fill up intramolecular bonding orbitals, the clusters are deformed by the Jahn–Teller effect. As a result, an intrinsic acceptor level, which is separated by 0.2 eV from the top of the valence band, is formed (5). It is believed that electrons due to metal doping occupy the intrinsic acceptor level. It has been reported that Li-doped β-r-B (Li_xB_{105}) showed an increase in electrical conductivity for $x \leq 5.7$ but a decrease for $x > 5.7$ (6). The changes in conductivity are explained by electron doping to the intrinsic acceptor level. On the other hand, electrical conductivity of V-doped β-r-B (V_xB_{105}) always increased with x (7). This change in conductivity cannot be explained by electron doping to the intrinsic acceptor level. Thus, the changes in the electronic structure of β-r-B caused by Li- and V-doping are different.

In the present study, the electronic structures of Li_xB_{105} ($x = 5.8$ and 7.9) and $V_{0.8}B_{105}$ are investigated using a high-resolution electron energy-loss spectroscopy (EELS) microscope (8, 9). We measured the band gap energy and volume plasmon energy. A characteristic difference between Li_xB_{105} and V_xB_{105} was observed in B K-shell excitation spectra (B K-edge).

EXPERIMENTAL

Li_xB_{105} ($x = 5.8$ and 7.9) were prepared by the reaction of Li vapor with polycrystalline β-r-B in an evacuated glass tube at 900–1000°C (6). $V_{0.8}B_{105}$ was prepared by melting the mixed powder of V and B and annealing at 1500°C (7). Electron diffraction patterns showed that the specimens examined were high-quality single crystals. EELS spectra were obtained from specimen areas of 180 nm in diameter with a thickness of about 100 nm by the high-resolution EELS microscope. The EELS microscope used was developed as a project of Joint Research with Industry by the Ministry of Education, Science, Sports, and Culture (8, 9). It is equipped with a thermal-type field emission gun as the electron source and specially designed double-focus Wien filters as the monochromator and analyzer. The illumination lens system, the specimen goniometer, and the imaging lens system of the EELS microscope are the same as the column part of a JEM1200EX transmission electron microscope. The EELS spectra were detected by a parallel-recording system with a charge-coupled device (CCD) camera. The best values of the full widths at half maximum (FWHM) of the zero-loss peak at present are 15 and 25 meV for the cases without and with a specimen, respectively. The accelerating voltage of incident electrons at the specimen was set at 60 kV. The retarding potential of the monochromator was set to be 51 V, and that of the analyzer 51–510 V.

RESULTS AND DISCUSSION

Figure 1 shows EELS spectra of Li_xB_{105} ($x = 5.8, 7.9$) and $V_{0.8}B_{105}$ in an energy range of 1–40 eV together with that of β-r-B for comparison. Energy resolutions of the spectra

0022-4596/97 $25.00

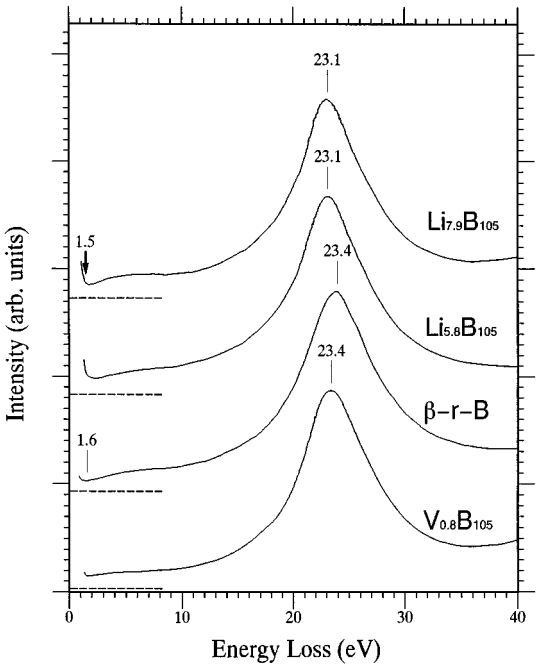

FIG. 1. Electron energy-loss spectra of Li_xB_{105} ($x = 5.8$ and 7.9) and $V_{0.8}B_{105}$ in an energy range of 1–40 eV together with that of β-r-B for comparison.

were 0.11–0.12 eV. The steep decrease of each spectrum around 1 eV is from the tail of the zero-loss peak. The spectrum onset of $Li_{7.9}B_{105}$ (band gap energy) was observed at about 1.5 eV, which is almost the same as that of β-r-B of 1.6 eV, as indicated by an arrow. The spectrum of $Li_{5.8}B_{105}$ did not show a clear onset. It was reported that electrical conductivity of Li_xB_{105} exhibited a maximum at $x = 5.8$ (7). Thus, it is considered that the onset of $Li_{5.8}B_{105}$ is smeared out by the superposition of a spectral intensity due to free carriers. The spectrum of $V_{0.8}B_{105}$, which has a larger electron conductivity than $Li_{5.8}B_{105}$, also did not show a clear onset. Prominent peaks are observed at 23.1 eV for Li_xB_{105} ($x = 5.8$ and 7.9) and 23.6 eV for $V_{0.8}B_{105}$. These peaks are due to the excitation of plasma oscillation of all valence electrons (volume plasmon). The energy of the volume plasmon decreases a little by Li- and V-doping. If the free electron model is assumed, Li- and V-doping (carrier doping) causes an increase of the volume plasmon energy. Thus, the decrease of the volume plasmon energy cannot be explained by the change in the density of valence electrons. The decrease should be affected by the change of interband transition energies due to Li- and V-doping.

The contribution of the direct beam was removed by a Lorentz fit and that of multiple scattering by the Fourier-log deconvolution method. The absolute value of the loss-function was calibrated by applying the sum rule. The dielectric function was derived from the loss-function by Kramers–Kronig analysis (KKA). The integrations with energy in the sum rule and in the KKA were carried out up to 400 eV, where the intensity profiles above 60 eV were obtained by extrapolating the profiles using an E^{-3} dependence. Figure 2 shows the real part, ε_1, and imaginary part, ε_2, of the

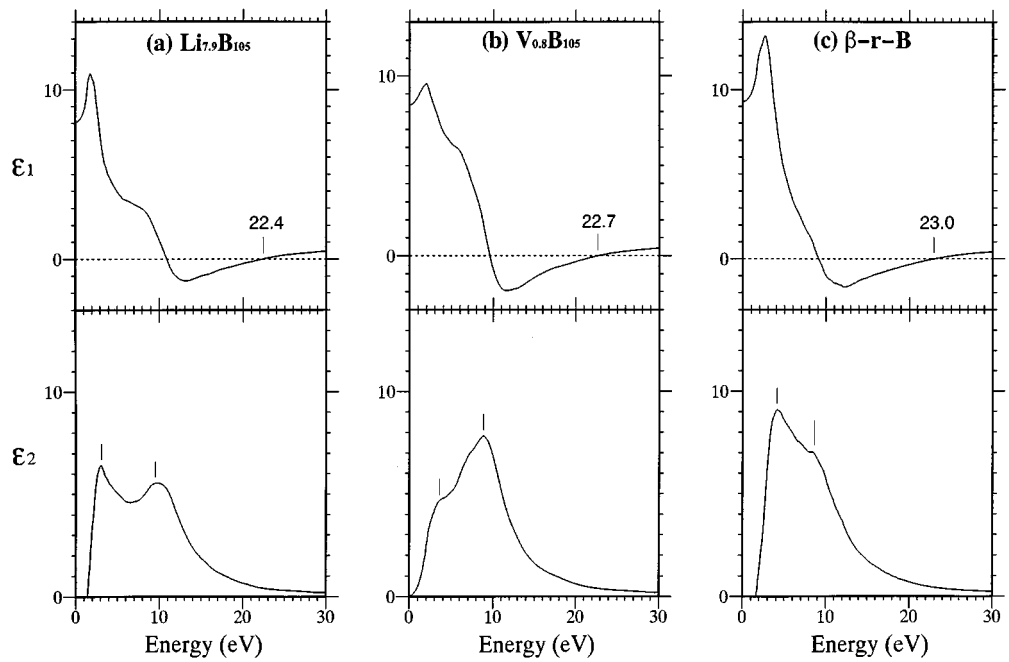

FIG. 2. Real part ε_1 and imaginary part ε_2 of the dielectric function of (a) $Li_{7.9}B_{105}$, (b) $V_{0.8}B_{105}$, and (c) β-r-B in an energy range of 0–30 eV.

dielectric function of (a) $Li_{7.9}B_{105}$, (b) $V_{0.8}B_{105}$, and (c) β-r-B in an energy range of 0–30 eV. The condition for the plasmon excitation, $\varepsilon_1 = 0$, is satisfied at 22.4 eV for $Li_{7.9}B_{105}$, 22.7 eV for $V_{0.8}B_{105}$ and 23.0 eV for β-r-B. This confirms that the peaks 23–24 eV in Fig. 1 correspond to the volume plasmon excitation. ε_2 of $Li_{7.9}B_{105}$ shows two broad peaks at about 3 eV and 10 eV. The 3 eV peak is more intense than the 10 eV peak, which is the same sense in ε_2 of β-r-B. ε_2 of $V_{0.8}B_{105}$ also shows two broad peaks at about 4 and 9 eV, but the sense of the relative peak intensity is opposite those of $Li_{7.9}B_{105}$ and β-r-B. This behavior indicates that the changes of the electronic structure are different between Li- and V-doping.

Figure 3 shows B K-edge of $Li_{7.9}B_{105}$, $Li_{5.8}B_{105}$, and $V_{0.8}B_{105}$ in an energy range of 185–195 eV together with that of β-r-B for comparison. Energy resolutions for the spectra were about 0.2 eV. Since these spectra were obtained under the condition of dipole transition, they show the partial density of states (DOS) with p characters in unoccupied states. The peak at 191.7 eV in the B K-edge of β-r-B shifts lower energy side with Li-doping. The energy onset did not change upon Li-doping, but the spectral intensity at about 178.5 eV increases. The increase may be caused by a change of the partial DOS with p characters due to the hybridization of the conduction band and Li 2s orbitals. The B K-edge of $V_{0.8}B_{105}$ shows the onset at 187.0 eV, which is lower than those of β-r-B and Li_xB_{105} by 0.9 eV. This indicates that the band gap energy of β-r-B decreases with V-doping. The decrease of the band gap energy may cause an increase in carriers thermally excited from the valence band to the conduction band. This may be the reason that the conductivity of V_xB_{105} always increases with x (7). Two broad peaks at 188.1 and 188.4 eV in the B K-edge of $V_{0.8}B_{105}$ may be caused by the mixing of the conduction band and the V 3d orbitals. It was reported that the doping sites of V atoms are tetrahedrally coordinated by the B_{12} clusters (6). Thus, the two peaks at 188.1 and 188.4 eV may be assigned respectively to e_g and t_{2g} levels of the V 3d state in a crystal field with tetragonal symmetry. Figure 4 schematically shows the changes of the electronic structure of β-r-B due to the Li- and V-doping. The present EELS spectra taken from one high-quality single quasicrystalline grain with a high energy-resolution provide important information about the electronic structures of the materials.

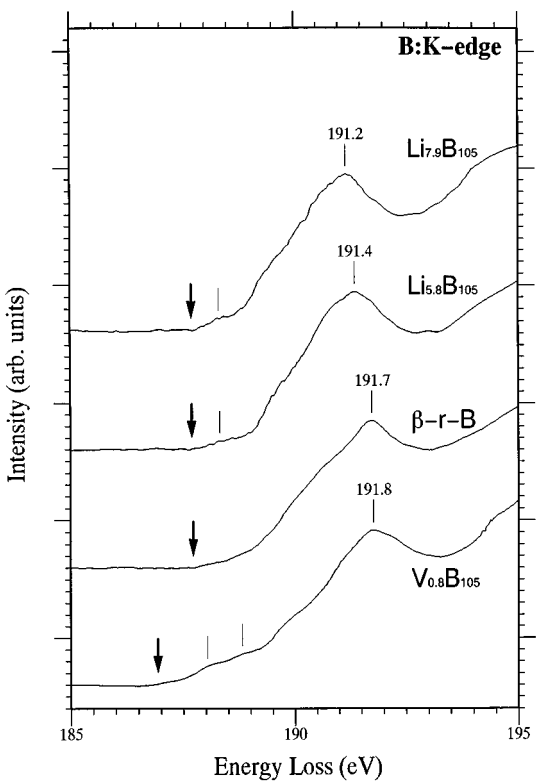

FIG. 3. B K-shell excitation spectra of Li_xB_{105} ($x = 5.8$ and 7.9) and $V_{0.8}B_{105}$ in an energy range of 185–195 eV together with that of β-r-B for comparison. Energy resolutions of the spectra were about 0.2 eV.

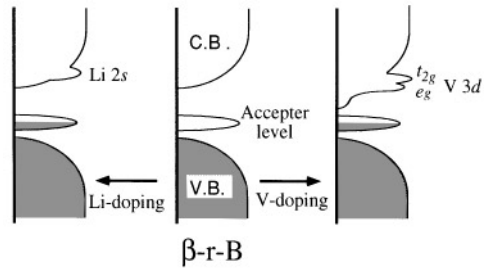

FIG. 4. Schematic picture of the changes of the electronic structure of β-r-B due to the Li- and V-doping. V.B. and C.B. indicate the valence band and the conduction band, respectively.

ACKNOWLEDGMENTS

The authors thank Dr. Y. Harada, Mr. M. Ishida, Dr. K. Tsuno, and Mr. M. Kai of JEOL Ltd. for their great effort in constructing the high-resolution EELS microscope. They thank Mr. F. Sato for his skillful technical assistance. The present work was partly supported by a Grant-in-Aid from the Ministry of Education, Science, Sports, and Culture, Japan.

REFERENCES

1. O. A. Golicova, *Phys. Stat. Sol.* **101,** 227 (1987).
2. I. Higashi, M. Kobayashi, Y. Akagawa, K. Kobayashi, and J. Bernhard, *AIP Conf. Proc.* **231,** 224 (1991).
3. M. F. Gaubauskas, J. S. Kasper, and G. A. Slack, *J. Solid State Chem.* **63,** 424 (1986).
4. M. Kobayashi, I. Higashi, H. Matsuda, and K. Kimura, *J. Alloy Comp.* **221,** 120 (1995).
5. R. Franz and H. Werheit, *AIP Conf. Proc.* **231,** 29 (1991).

6. H. Matsuda, T. Nakayama, K. Kimura, Y. Murakami, H. Suematsu, M. Kobayashi, and H. Higashi, *Phys. Rev. B* **52,** 6102 (1995).
7. H. Matsuda, N. Tanaka, T. Nakayama, K. Kimura, Y. Murakami, H. Suematsu, M. Kobayashi, and H. Higashi, *J. Phys. Chem. Solids* **57,** 1167 (1996).
8. M. Terauchi, R. Kuzuo, F. Satoh, M. Tanaka, K. Tsuno, and J. Ohyama, *Microsc. Microanal. Microstruct.* **2,** 351 (1991).
9. M. Tanaka, M. Terauchi, R. Kuzuo, K. Tsuno, J. Ohyama, and Y. Harada, "Proceedings, 50th Annual Meeting of Electron Microscopy Society of America," San Francisco Press, San Francisco, p. 940, 1992.